



## Anatase-3DOM Structure for Reactive Red Dye Photocatalytic Degradation

 Tanya Kiatboonyarit <sup>1\*</sup>, Thipchanok Bowornhathai <sup>1</sup>, Ramida Rattanakam <sup>1</sup>, Supakit Achiwawanich <sup>1</sup>, Sutasinee Kityakarn <sup>1\*</sup>
<sup>1</sup> Department of Chemistry, Faculty of Science, University of Kasetsart, Bangkok, Thailand, 10903.

\*Corresponding author's e-mail address: fscistsn@ku.ac.th

### ARTICLE INFO

#### Article history

Submitted: 24 March 2017

Revised: 5 April 2017

Accepted: 10 July 2017

Available online: 28 July 2017

#### Keywords:

Ce-doped TiO<sub>2</sub>TiO<sub>2</sub>

3DOM

Dye degradation

Photocatalysts

© 2017 The Microscopy Society of Thailand

### ABSTRACT

Photocatalysts TiO<sub>2</sub>-powder and TiO<sub>2</sub>-3DOM (Three-dimensionally ordered macroporous, 3DOM) were prepared by the sol-gel method and calcined at 723 K. The TiO<sub>2</sub> and Ce/TiO<sub>2</sub> photocatalysts showed only anatase phase without CeO<sub>2</sub> and the particle size of the Ce/TiO<sub>2</sub>-3DOM was smaller than the TiO<sub>2</sub>-powder. The Poly(methyl methacrylate, PMMA) was the template for TiO<sub>2</sub> particle-orientation as investigated by SEM. The stoichiometry of element and the molar percentage of Ce/Ti in the sample were determined by EDS. The photocatalytic degradation of reactive red dye was evaluated by UV-Vis spectroscopy. TiO<sub>2</sub>-powder-723 showed the highest photocatalytic activity compared to others due to their morphology and particle size.

## INTRODUCTION

Wastewater from textile industrial processes generally consists of surfactants, chelating reagents, pH regulators, dyes and etc. Azo dyes are commonly used in the dyeing process. The residual dyes are biologically non-degradable compounds that contaminate wastewater. In textile wastewater treatment, color removal is a primary concern. Several methods such as electrocoagulation methods, electrochemical reduction methods, electrochemical oxidation methods, indirect oxidation methods and photo-assisted methods have been applied in order to eliminate dyes from wastewater [1-3].

The photo-Fenton process is the photoassisted method where H<sub>2</sub>O<sub>2</sub>, iron sulfate and UV radiation are incorporated resulting in OH· radicals which are capable of reducing harmful organic compounds. For the heterogeneous photocatalysis method, TiO<sub>2</sub> is used in the advanced oxidation process (AOP) for the mineralization of many organic pollutants. TiO<sub>2</sub> is a photoactive semiconductor, and generates electron/hole pairs (e<sup>-</sup>/h<sup>+</sup>) when irradiated by photons with sufficient energy. The generated e<sup>-</sup>/h<sup>+</sup> pairs react with water or oxygen producing OH· or O<sub>2</sub>· radicals, which will then react with the organic compounds to break them down to CO<sub>2</sub> and H<sub>2</sub>O.

The improvement of photocatalysts is essential to reach the full potential of solar radiation because most photocatalysts are excited by UV radiation which accounts for only a small percentage of sunlight. The doping or substituting of p-block, lanthanide or actinide elements into TiO<sub>2</sub> such as Pt-TiO<sub>2</sub>, B-TiO<sub>2</sub>, CeO<sub>2</sub>-TiO<sub>2</sub>, [4,5-14] is interesting for researchers. The application of rare earth elements like Ce (Ce<sup>3+</sup>/

Ce<sup>4+</sup>) is able to suppress the recombination of e<sup>-</sup>/h<sup>+</sup> pairs and increases the efficiency of TiO<sub>2</sub> photocatalysts by decreasing the band-gap energy. In addition, the morphology of photocatalysts is important to modify the efficiency of photocatalysts.

In this research, TiO<sub>2</sub> and Ce/TiO<sub>2</sub> photocatalysts with different morphologies (powder and 3DOM) were prepared by the sol-gel method. The 3DOM formation of TiO<sub>2</sub> was prepared using PMMA as a template. The effect of Ce addition and the morphology of TiO<sub>2</sub> were investigated. The photocatalytic degradation of reactive red dye (RR) was evaluated by UV-Vis spectroscopy.

## METHODOLOGY

Titanium (IV) isopropoxide, ethanol and cerium (III) nitrate hexahydrate were used for sol-gel preparation. The gelation of samples was at 323 K for 24 h and heated up to 383 K for 24 h. The dry powder was calcined at 723 K and 873 K under the mixing of N<sub>2</sub> and O<sub>2</sub> (70:30), (labeled, respectively, as TiO<sub>2</sub>-powder-723 and TiO<sub>2</sub>-powder-823). The sample with Ce was prepared by adding 2% molar ratio of Ce to Ti into the mixture (labeled as 2%Ce/TiO<sub>2</sub>-powder-723).

The 3DOM samples were prepared in the same manner. TiO<sub>2</sub>-powder and the mixture of Ce/TiO<sub>2</sub> was prepared by the addition of cerium (III) nitrate solution with 2% molar ratio of Ce to Ti. The mixture was dropped onto the PMMA, kept at room temperature for 7 days, dried at 353 K for 12 h and calcined at 723 K under the mixing of N<sub>2</sub> and O<sub>2</sub> (70:30) and the samples were labeled as TiO<sub>2</sub>-3DOM, and 2%Ce/TiO<sub>2</sub>-3DOM.

The structure of all the samples was characterized by X-ray diffraction spectrometer (XRD, D8 Advance Bruker). The  $\text{Cu } K_{\alpha}$  x-ray is generated by an x-ray tube operated at 40 kV and 30 mA. The XRD patterns were recorded in the range of 10-80 degree. The XRD patterns were indexed by comparison with the JCPDS file. The morphology of the samples and the chemical composition in the prepared samples were investigated by Scanning Electron Microscope (SEM) equipped with energy dispersive X-ray spectrometer (EDS), Quanta 450FEI. The samples were sputtered with Au and imaged at 10k and 30k magnification. The photocatalytic dye degradation by  $\text{TiO}_2$  catalysts was evaluated using UV-Vis spectroscopy. The suspended  $\text{TiO}_2$  photocatalysts in the 12 ppm RR dye solution were irradiated by UV source (B-100YP, UVP lamp). The adsorption at 541 nm was used to determine the photocatalytic degradation of RR dye.

## RESULTS AND DISCUSSION

The XRD patterns of all samples in Figure 1 showed the pattern of  $\text{TiO}_2$  anatase (PDF No. 01-075-2545) without other  $\text{TiO}_2$  phases and  $\text{CeO}_2$  (PDF No. 01-078-3080). The  $\text{TiO}_2$ -powder-823 showed highly sharp intensity indicating the high crystallinity of the  $\text{TiO}_2$  anatase. The  $\text{TiO}_2$ -commercial,  $\text{TiO}_2$ -powder-723 and 2%Ce/ $\text{TiO}_2$ -powder-723 showed broad XRD peaks indicating the small crystalline size of the  $\text{TiO}_2$  anatase. The  $\text{TiO}_2$ -3DOM-723 and 2%Ce/ $\text{TiO}_2$ -3DOM-723 showed boarder peaks and lower intensity of anatase phase due to the small crystalline size of  $\text{TiO}_2$  anatase forming in 3DOM structure. The addition of Ce in the  $\text{TiO}_2$  structure did not deform the anatase phase, however it suppressed the growing of  $\text{TiO}_2$  crystal, resulting in the small crystalline size. The XRD peak intensity was affected by Ce addition. The high percentage of Ce showed a low XRD intensity indicating that the cerium ions dissolved in anatase phase [12]. This means that the Ce addition percentage represented the cerium ion solubility in anatase.

The morphology and chemical composition of  $\text{TiO}_2$  photocatalysts were evaluated by SEM- EDS (Figure 2 and Table1). The SEM

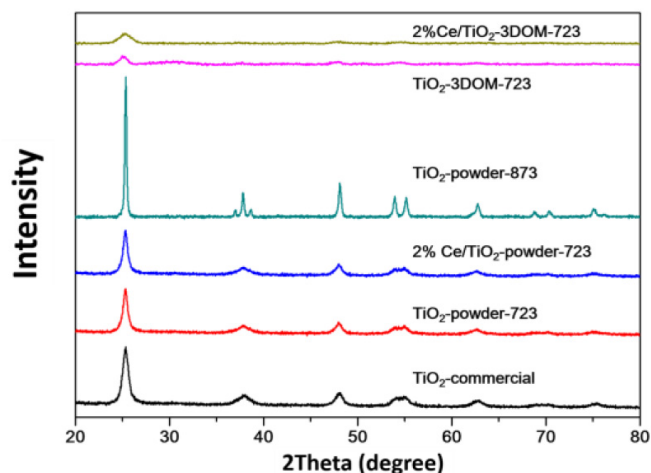
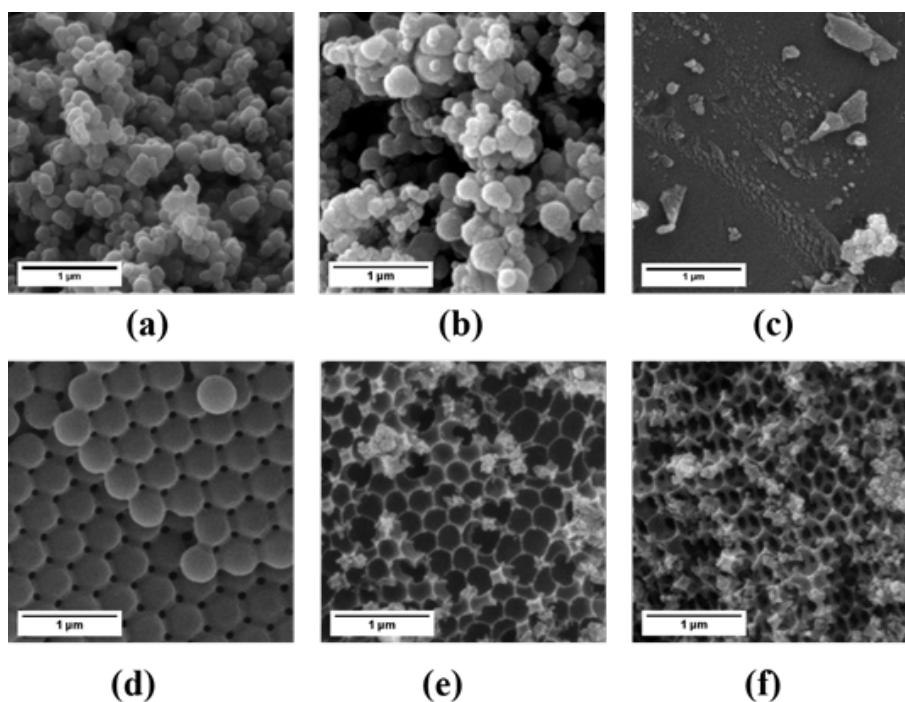


**Figure 1** XRD patterns of  $\text{TiO}_2$ -commercial,  $\text{TiO}_2$ -powder-723, 2%Ce/ $\text{TiO}_2$ -powder-723,  $\text{TiO}_2$ -powder-873,  $\text{TiO}_2$ -3DOM-723 and 2%Ce/ $\text{TiO}_2$ -3DOM-723.

images presented the small particle size of  $\text{TiO}_2$ -commercial and  $\text{TiO}_2$ -powder-723 which correspond to the board XRD peaks (Figure 2 (a) – (b)). 2%Ce/ $\text{TiO}_2$ -powder-723 showed smaller, compact particles compared to the other powders (Figure 2 (c)). The percentage molar ratio of Ce to Ti in 2%Ce/ $\text{TiO}_2$ -powder-723 was 2.2 %.

The particles of PMMA were spherical with size of approximately 0.25  $\mu\text{m}$ , Figure 2 (d). PMMA was used as the template for 3DOM formation for  $\text{TiO}_2$  prepared by the sol-gel method. After the mixture of  $\text{TiO}_2$  precursor was dropped onto the surface of PMMA and the coated  $\text{TiO}_2$  precursor decomposed at 723 K,  $\text{TiO}_2$  anatase with 3DOM structure and small particles  $\text{TiO}_2$  anatase formed on the 3DOM structure as shown in Figure 2 (e) – (f).

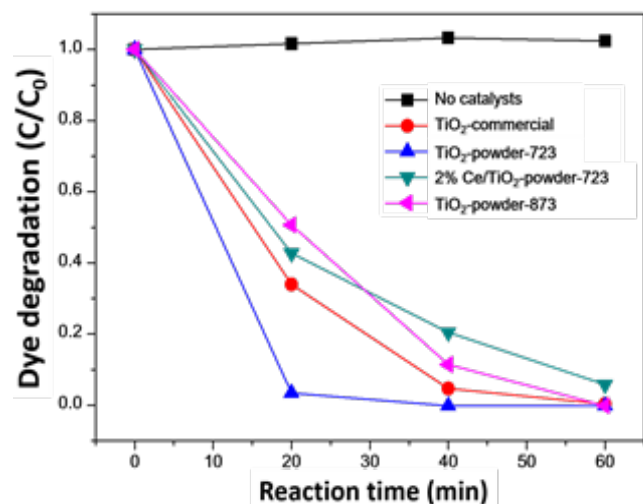
The particle sizes of  $\text{TiO}_2$ -3DOM-723 and 2%Ce/ $\text{TiO}_2$ -3DOM-723 were small and their morphology was more regular



**Figure 2** SEM images of (a)  $\text{TiO}_2$ -commercial, (b)  $\text{TiO}_2$ -powder-723, (c) 2%Ce/ $\text{TiO}_2$ -powder-723, (d) PMMA, (e)  $\text{TiO}_2$ -3DOM-723 and (f) 2%Ce/ $\text{TiO}_2$ -3DOM-723. The magnification of all sample was 30k and scale bar was 1  $\mu\text{m}$ .

**Table 1** Chemical composition of photocatalysts measured by EDS.

Photocatalysts	Elemental (weight %)			Elemental (atomic %)		
	Ti	Ce	O	Ti	Ce	O
TiO <sub>2</sub> -commercial	56.92		43.08	30.62		69.38
TiO <sub>2</sub> -powder-723	57.34		42.66	30.98		69.02
2%Ce/TiO <sub>2</sub> -powder-723	54.70	3.65	41.65	30.28	0.69	69.03
TiO <sub>2</sub> -3DOM-723	61.63		38.37	34.91		65.09
2%Ce/TiO <sub>2</sub> -3DOM-723	56.12	5.25	38.63	32.33	1.03	66.64

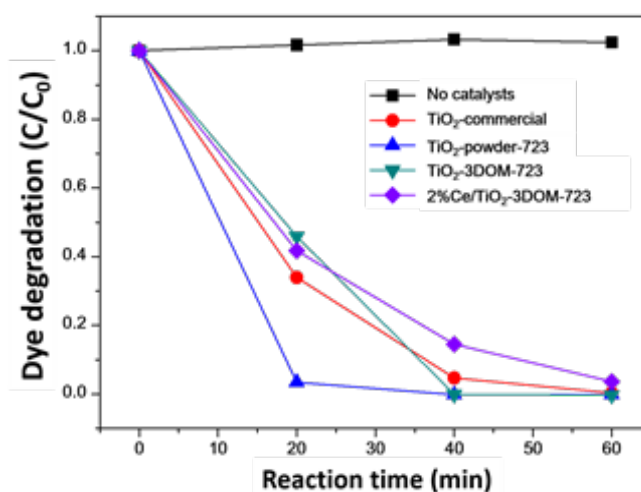
**Figure 3** Photocatalytic activity of non-catalysts, TiO<sub>2</sub>-commercial, TiO<sub>2</sub>-powder-723, 2%Ce/TiO<sub>2</sub>-powder-723, TiO<sub>2</sub>-powder-873.

than the 2%Ce/TiO<sub>2</sub>-powder-723. The SEM image of TiO<sub>2</sub>-3DOM showed agglomeration of TiO<sub>2</sub> on the 3DOM structure. The number of agglomerated particles increased with the addition of Ce resulting in deformation of 3DOM structure as observed in Figure 2 (f). The percentage molar ratio of Ce to Ti in 2%Ce/TiO<sub>2</sub>-3DOM was 3.1%.

The photocatalytic degradation of reactive red dye (RR) by TiO<sub>2</sub>-anatase under irradiation was investigated by sampling 2 mL of solution every 20 min; the results are shown in Figure 3 and Figure 4. The RR dye did not degrade under irradiation without catalysts. The TiO<sub>2</sub>-powder-723 showed the highest dye photodegradation due to its small regular particles. The TiO<sub>2</sub>-powder-873 showed low catalytic activity compared to the TiO<sub>2</sub>-powder-723 despite having the highest crystallinity of anatase phase. It is well known that the agglomeration of TiO<sub>2</sub> particles take place at high calcination temperature, resulting in large particle size and decreased surface area of catalysts. The photocatalytic activity of Ce added into TiO<sub>2</sub> was not significantly different from the TiO<sub>2</sub>-powder-873. However, the photocatalytic activity of Ce/TiO<sub>2</sub> was lower than the TiO<sub>2</sub>-powder-723 and TiO<sub>2</sub>-commercial. This was due to the small compact particles of Ce/TiO<sub>2</sub>-powder-723, which lead to decreased surface area of catalysts and lower catalytic activity.

To study the effect of morphology of TiO<sub>2</sub> photocatalysts with different morphology were used. The photodegradation of RR by TiO<sub>2</sub>-3DOM-723 and 2%Ce/TiO<sub>2</sub>-3DOM-723 showed similar photocatalytic activity that was lower than the TiO<sub>2</sub>-powder-723 due to smaller photocatalysts particle sizes.

In further research, the preparation of 3DOM at high calcination temperature will be considered and the photocatalytic activity of high temperature calcined 3DOM will be investigated. The decrease in cerium percentage will be studied in order to evaluate the threshold of cerium present in the TiO<sub>2</sub> structure, which can enhance the

**Figure 4** Photocatalytic activity of non-catalysts, TiO<sub>2</sub>-commercial, TiO<sub>2</sub>-powder-723, TiO<sub>2</sub>-3DOM-723, 2%Ce/TiO<sub>2</sub>-3DOM-723.

photocatalytic activity of TiO<sub>2</sub>.

## CONCLUSION

The anatase-3DOM was prepared by sol-gel method and PMMA was used as a template for 3DOM formation. The addition of Ce suppressed the growing of TiO<sub>2</sub> particles, resulting in small particles of Ce/TiO<sub>2</sub> for both powder and 3DOM. The TiO<sub>2</sub>-powder-723 showed the highest photocatalytic activity due to its small regular particles. The addition of Ce into TiO<sub>2</sub> did not improve the photocatalytic activity of TiO<sub>2</sub> catalysts. The anatase 3DOM structure exhibited low photocatalytic activity due to the smaller particle size of the catalyst and lower degree of TiO<sub>2</sub> crystallinity. Increased calcination temperature was considered to enhance the photocatalytic activity of TiO<sub>2</sub>-3DOM.

## ACKNOWLEDGEMENTS

Financial support by Kasetsart University Research and Development Institute and Department of Chemistry, Faculty of Science, Kasetsart University are fully acknowledged.

## References

- O. Ercan, S. Deniz, E.K. Yetimoglu and A. Aydin, Degradation of Reactive Dyes Using Advanced Oxidation Method, *Clen-Soil, Air, Water*, **2015**, 7, 1031-1036.
- N. T. Dung, N.V. Khoa and J.-M. Herrmann, Photocatalytic Degradation of Reactive Dye RED-3BA in Aqueous TiO<sub>2</sub> Suspension under UV-Visible Light, *Iner.J. Photoenergy*, **2005**, 7, 11-15.
- M. Sala and M.C. Gutierrez-Bouzan, Electrochemical Techniques in Textile Process and Wastewater Treatment, *Inter.J.Photoenergy*,

- 2012, 1-12.
4. A.A. Ismail and D.W. Bahnemann, Photochemical splitting of water for hydrogen production by photocatalytic: A Review, *Sol. Energ. Mat. Sol. C.*, **2014**, 128, 85-101.
  5. W. Wang, M.O. Tade and Z. Shao, Research progress of perovskite materials in Photocatalysis- and Photovoltaics-related energy conversion and environmental treatment, *Chem.Soc.Rev.*, **2015**, 44, 5371-5408.
  6. S. G. Kumar and L.G. Devi, Review on Modified TiO<sub>2</sub> Photocatalysis under UV/Visible Light: Selected Results and Related Mechanisms on Interfacial Charge Carrier Transfer Dynamics, *J.Phys.Chem. A*, **2011**, 115, 13211-13241.
  7. W. Chao-hai, T. Xin-hu, L. Jie-rong and T. Shu-ying, Preparation, Characterization and Photocatalytic activities of Boron- and Cerium- doped TiO<sub>2</sub>, *J. Environ. Sci.*, **2007**, 19, 90-96.
  8. M. Tian, H. Wang, D. Sun and W. Peng, Visible Light Driven Nanocrystal anatase TiO<sub>2</sub> Doped Ce from Sol-gel Method and its Photoelectrochemical Water Spilling Properties, *Int. J. Hydrogen Energ.*, **2014**, 39, 13448-13453.
  9. M. Zou, Y. Kong, J. Wang, Q. Wang, Z. Wang, B. Wang and P. Fan, Spectroscopic Analyses on ROS Generation Catalyzed by TiO<sub>2</sub>, CeO<sub>2</sub>/TiO<sub>2</sub> and Fe<sub>2</sub>O<sub>3</sub>/TiO<sub>2</sub> under Ultrasonic and Visible-light irradiation *Spectrochim. Acta. A.*, **2013**, 101, 82-90.
  10. L. Matejova, V. Vales, R. Fajgar, Z. Matej, V. Holy and O. Solcova, Reverse Micelles Directed Synthesis of TiO<sub>2</sub>-CeO<sub>2</sub> Mixed Oxide and Investigation of their Crystal Structure and Morphology, *J. Solid State Chem.*, **2013**, 198, 485-495.
  11. A. Niltarach, S. Kityakarn, A. Worayingyong, J. T-Thienprasert, W. Klysubun, P. Songsiririttingul, S. Limpijumnong, Structural Characterizations of Sol-gel Synthesized TiO<sub>2</sub> and Ce/TiO<sub>2</sub>